Talanta 130 (2014) 415–422

Contents lists available at ScienceDirect

Talanta

journal homepage: www.elsevier.com/locate/talanta

L-cysteine protected copper nanoparticles as colorimetric sensor for mercuric ions

Razium A. Soomro [a,*], Ayman Nafady [b], Sirajuddin [a], Najma Memon [a], Tufail H. Sherazi [a], Nazar H. Kalwar [a]

[a] National Centre of Excellence in Analytical Chemistry, University of Sindh, Jamshoro 76080 Pakistan
[b] Department of Chemistry, College of Science, King Saud University, Riyadh 11451, Saudi Arabia

ARTICLE INFO

Article history:
Received 30 April 2014
Received in revised form
8 July 2014
Accepted 9 July 2014
Available online 22 July 2014

Keywords:
Copper nanoparticles
L-cysteine
Colorimetric sensor
Mercuric ions
Amino acid

ABSTRACT

This report demonstrates a novel, simple and efficient protocol for the synthesis of copper nanoparticles in aqueous solution using L-cysteine as capping or protecting agent. UV–visible (UV–vis) spectroscopy was employed to monitor the LSPR band of L-cysteine functionalized copper nanoparticles (Cyst-Cu NPs) based on optimizing various reaction parameters. Fourier Transform Infrared (FTIR) spectroscopy provided information about the surface interaction between L-cysteine and Cu NPs. Transmission Electron Microscopy (TEM) confirmed the formation of fine spherical, uniformly distributed Cyst-Cu NPs with average size of 34 ± 2.1 nm. X-ray diffractometry (XRD) illustrated the formation of pure metallic phase crystalline Cyst-Cu NPs. As prepared Cyst-Cu NPs were tested as colorimetric sensor for determining mercuric (Hg^{2+}) ions in an aqueous system. Cyst-Cu NPs demonstrated very sensitive and selective colorimetric detection of Hg^{2+} ions in the range of 0.5×10^{-6}–3.5×10^{-6} mol L^{-1} based on decrease in LSPR intensity as monitored by a UV–vis spectrophotometer. The developed sensor is simple, economic compared to those based on precious metal nanoparticles and sensitive to detect Hg^{2+} ions with detection limit down to 4.3×10^{-8} mol L^{-1}. The sensor developed in this work has a high potential for rapid and on-site detection of Hg^{2+} ions. The sensor was successfully applied for assessment of Hg^{2+} ions in real water samples collected from various locations of the Sindh River.

1. Introduction

Recently, considerable scientific interest has been focused on the fabrication and application of metal nanoparticles (NPs). The diversity of metal NPs in shapes and diminutive sizes has allowed researchers to explore their captivating applications in fields like catalysis, electronics, sensors, optical devices and biotechnology. Metal nanoparticles particularly, gold (Au), silver (Ag) and copper (Cu) have drawn tremendous attention over other metals due to their most unique and fascinating property known as Localized Surface Plasmon Resonance (LSPR) [1]. When the size of metal particles diminishes to nano scale regime, a strong UV–vis excitation band is observed due to collective oscillation of conducting band electron at metal surface. Unlike the customary UV–vis band, this LSPR of metal nanoparticles is the characteristics of nano scale size and demonstrates extreme sensitivity towards the shape, size, and composition of metal under study [2]. Nobel metal NPs like Au, Ag and Cu within the size range of 10–60 nm exhibit LSPR band around 520 nm, 400 nm, and 570 nm, with magnificent purple, yellow, and red colloidal color, respectively [3–6]. In particular, LSPR property of metal nanoparticle strongly depends on the inter particle distance between the aggregated nanoparticles, thus allowing LSPR based metal absorption to be used as an analytical property for optical and colorimetric sensing of various chemical species with low cost, simplicity and sensitivity [7].

At present much of research attention concerning the preparation and application of plasmonic nanostructures is paid to precious metals like Au and Ag. However, the high cost margin and hence difficult availability of these metals restrict the development of economic sensors for on site assessment besides their usage in large volume production [8]. In such connection, Cu with LSPR band residing within the visible region of electromagnetic spectrum, lower cost, and easy availability as compared to Au and Ag can serve as a suitable alternative. Recently, Hatamie et al. [9] have reported the use LSPR of Cu nanoparticles for selective and sensitive colorimetric detection of sulfide ions (S^{2-}) up to micromolar concentration. However, since in the mentioned report Cu nanoparticles were obtained via CTAB assisted reduction route in

* Corresponding author. Tel.: +92 336 3051253; fax: +92 22 9213431.
E-mail address: raziumsoomro@gmail.com (R.A. Soomro).

http://dx.doi.org/10.1016/j.talanta.2014.07.023
0039-9140/

capped bottle, poor efficiency of CTAB would still result in oxide formation in open air. Unfortunately, very less attention has been paid towards the fabrication of pure Cu nanoparticles for plasmonic application. The major problem associated with utilizing Cu nanoparticles as plasmonic sensors is their tendency to oxidize within the aqueous environment, other than rapid agglomeration and desire for large quantities of synthesized product. To surmount these problems, numerous strategies have been proposed including the use of non-aqueous solvent system, synthesis and storage under inert atmosphere and use of suitable stabilizers like surfactants and polymers. Vaseem et al. [10] reported synthesis of Cu nanoparticles employing CTAB as a stabilizing agent and N_2H_2 as a reducing agent, where production of N_2 by-product from hydrazine avoided the use of protecting gases. Similarly, Lai et al. [11] prepared Cu nanoparticles with the application of polymer like (PVP) and NaH_2PO_2 without using any protective gas. However, synthetic procedure was time consuming and took a long time of seventeen hours with heat requirement. Zhang et al. [12] prepared Cu nanoparticles using gelatin as capping agent. Since gelatin is less soluble in water at room temperature, it would have been difficult to re-disperse the particles in water. Hence, a more convenient and reliable method for synthesis of Cu nanoparticles in aqueous system is still a challenge.

In context with the application of LSPR based materials, sensitive and selective chemo sensors broadly used for the determination of heavy metal ions have been considerably attended in order to disclose their toxic effects. Among such metals, mercury is considered as one of the most important toxic metal in the form of mercuric (Hg^{2+}) ion for environment and humans because of its wide distribution in various metallics and organic and inorganic forms that are found in air, water and soil [13–15]. Due to its higher water solubility, Hg^{2+} ion is considered as the most stable form of inorganic mercury, which can easily exist in surface waters and can cause several health related issues including damage to brain, kidneys, and the nervous system [16,17]. The various classical instrument based determination methods include atomic absorption/emission spectrometry (AAS/AES) [18–20], inductively coupled plasma mass spectrometry (ICPMS) [21,22], high-performance liquid chromatography (HPLC) [23], atomic fluorescence spectrometry (AFS) [24], flame photometry (FP) and ion selective electrode (ISE) [25]. These techniques although powerful and efficient for heavy metal ion determination, suffer from drawbacks like highly expensive instrumentation, time consuming sample preparations and inability to be used as on-site monitoring feasible techniques. In comparison, colorimetric based methods can provide rapid naked eye detection, appropriate on site assessment capability, real time analysis of target metal ion due to simple configuration and portability to be used on site [26]. To date, Au and Ag nanoparticles have been extensively employed as colorimetric detectors for heavy metal ions in the aqueous phase due to their excellent LSPR characteristics allowing easy visualization of color change [7]. Solanki et al. [27] reported a simple colorimetric detection method for Hg^{2+} and Pb^{2+} ions based on metal ions-peptide complex inducing the aggregation of Au NPs. Similarly Bothra et al. [28] developed p-phenylenediamine (p-PDA) functionalized Ag NPs for the sensitive colorimetric determination of Hg^{2+} and Fe^{2+} in aqueous medium. Liu et al. [29] showed highly sensitive and selective colorimetric detection of Hg^{2+} ion based on the aggregation of quaternary ammonium group-capped gold nanoparticles caused by abstraction of thiols from the surface of gold nanoparticles. In contrast colorimetric determination based chemical reaction between green synthesized Ag NPs and Hg^{2+} ions has also been reported by Farhadi et al. [8].

The protection of some cost effective metal nanoparticles via their stabilization against oxidation is the need of the day in order to develop cheaper but still efficient products for various tasks. In the previous work, our group fabricated stable nickel nanoparticles using L-threonine [30] and L-cysteine [31] as protecting agents and used them in the field of catalysis. In continuation of the similar strategy in order to make the task extremely economic, efforts were made to use L-cysteine as the capping or protecting agent for synthesis of Cu nanoparticles against oxidation in aqueous phase. These stable Cu nanoparticles were successfully utilized as sensitive and selective colorimetric sensor for Hg^{2+} ions in both control experiments and real water samples collected from the River Sindh near Kotri Barrage Jamshoro, Hyderabad, Pakistan. The use of amino acid (L-cysteine) as protecting agent is a greener approach for synthesis of Cu nanoparticles. Furthermore, this strategy extremely economizes the process as compared to similar sensing of Hg^{2+} ions via precious metals, Au or Ag.

2. Experimental

2.1. Materials and reagents

All chemicals used were of analytical grade and used without further purification by employing pure Milli-Q water as the preparatory medium. $CuCl_2 \cdot 5H_2O$ (97%), hydrazine hydrate ($N_2H_4 \cdot H_2O$), (80%), were obtained from E. Merck, L-cysteine ($C_3H_7NO_2S$), from Fluka Chemicals. NaOH (98%), HCl (37%), and different salts including $MgCl_2 \cdot 6H_2O$, $Ca(NO_3)_2 \cdot 4H_2O$, $Pb(NO_3)_2$, $Zn(NO_3)_2 \cdot 6H_2O$, $Co(NO_3)_2 \cdot 6H_2O$, $Ni(NO_3)_2 \cdot 6H_2O$, $Mn(NO_3)_2 \cdot 4H_2O$, $Cd(NO_3)_2$, $AgNO_3$ and $HgSO_4 \cdot H_2O$ were purchased from Sigma-Aldrich. The stock solutions of metal ions were prepared by dissolving a known amount (per mg) of each salt in pure Milli-Q water and all experiments were performed at ambient temperature (25 ± 2 °C).

2.2. Instrumentation

UV–visible spectroscopy (Lambda 35 of Perkin-Elmer) was used for tracing LSPR of Cyst-Cu NPs and performing colorimetric assay measurements within the spectral range of 400–800 nm. Surface fictionalization of Cu NPs with L-cysteine was observed by Fourier transform infrared (FTIR) spectroscopy (Nicolet 5700 of Thermo) using the KBr pelleting method. Solid sample were obtained, after parching colloidal dispersion of Cyst-Cu NPs under nitrogen atmosphere. Morphological characterization for size distribution and shape homogeneity of colorimetric sensor (Cyst-Cu NPs) before and after the colorimetric assay was performed using TEM (Jeol JEM 1200 EX MKI). Similarly changes in phase composition of the colorimetric sensor were studied using an XRD model D-8 of Bruker. Photographs of the colloidal Cyst-Cu NPs used for visual colorimetric detection of Hg^{2+} were recorded by using a digital camera.

2.3. Procedure for synthesis of copper nanoparticles

The synthesis of Cyst-Cu NPs was achieved in a capped test tube of 10 mL volume capacity. In a typical synthetic procedure, 300 μL of 0.003 M solution of $CuCl_2$, was diluted with de-ionized water up to 08 mL taken in a 10 mL test tube. To this was added 20 μL of 0.01 M L-cysteine solution which turned the color of mixture from light blue to colorless. This was followed by addition of 1000 μL of 0.1 M hydrazine monohydrate ($N_2H_4 \cdot H_2O$) for reduction of metal ions during which the solution mixture changed from colorless to red within 60 min of reaction time. The pH of entire mixture was maintained at 6.5 in accordance to pk_a values of L-cysteine to get hold of the smallest particle size.

The change in color indicated the formation of Cu NPs and the resulting product was used for colorimetric assay. The use of hydrazine monohydrate as a mild reducing agent allowed preserving homogeneity of synthesized nanoparticles with generation of an inert atmosphere, making this protocol independent from the use of protective gas and hence tedious strategies to avoid oxidation.

2.4. Colorimetric sensing of Hg^{2+} ions by cyst-Cu NPs

The colorimetric detection of aqueous Hg^{2+} ions was performed at room temperature. Briefly, 10 μl of Hg^{2+} ions with different concentrations ranging from 0.5 to 3.5 μM were added to 3 ml of Cyst-Cu NPs solution. These solutions were mixed slowly for 2–3 min followed by transfer of small portion into a 1 cm quartz cell to record absorbance. Absorbance was measured at LSPR wavelength of 565 nm, against a blank reagent. ΔA (LSPR) was used as the analytical signal and color changes from light red to pale yellow taken as a naked eye colorimetric response of system. The corresponding color changes were recorded with an 18 mega pixel digital camera after mixing the solution for 2 min.

2.5. Use of cyst-Cu NPs as sensor for assay of Hg^{2+} ions in real water samples

Three samples were collected from various localities of the river Sindh near Kotri barrage. The samples were filtered, and two times diluted before performing analytical assay. These samples were treated in the same way as true in case of Hg^{2+} ions detection in standard using Cyst-Cu NPs as colorimetric sensors.

3. Results and discussion

3.1. Spectroscopic characterization of functionalized Cu NPs

In recent years, several studies have shown that optical properties of metal nanoparticles depend upon the geometry and size; thus the optical response of metal nanoparticles (NPs) can be tuned to control shape and size of metal nanostructure [32–34]. Since surface plasmon modes of metallic nanoparticles like Au, Ag and Cu, reside within the optical region of electromagnetic spectrum [35,36], optical spectroscopy was used as a primary tool for investigation of Cyst-Cu nanoparticles. Visible spectral profiles were recorded for optimization of various reaction parameters like concentration of copper chloride, L-cysteine, hydrazine, and pH of solution. The most stable and small sized Cyst-Cu NPs (with blue-shifted spectrum) were obtained by taking appropriate concentrations of the precursor salt solutions. Experimental results provided in Fig. S1(a) (Supplementary data) show an increase in absorbance parallel to very slight shift in LSPR band wavelength with greater amount of Cu ions (0.1–0.8 ml of 0.003 M). However, with a higher amount of precursor Cu ions ⩾0.8 mL, precipitation occurred with disappearance of the LSPR band. The color intensity of Cyst-Cu NPs was noted to vary in order with concentration of Cu ions as shown in the inset digital photograph. This increase in LSPR absorbance may be defined as the consequence of increased nucleation rate with greater Cu (II) ions available in solution generating smaller nanoparticles as reported elsewhere [37,38].

Visible spectral profile, (Fig. S1(b)) based on optimization of reducing agent (50–200 μl of 0.001 M) suggests reduced particle size as evident from the shift in LSPR wavelength from 577 nm to a shorter wavelength of 567 nm. This trend in spectral profile is owing to diminished number of solute per growing particle as the number of nuclei produced per single nucleation period increases [38]. It is interesting to note that visible spectral profile (Fig. S1(c)) based on increasing concentration of functionalizing or protecting agent (L-cysteine), shows change in LSPR band shape and a blue-shift from 567 nm to 565 nm with increasing concentration of L-cysteine. Decreased broadening of LSPR band may be ascribed to the uniform particles size (homogenous) distribution within the sample solution. In general, an increase in concentration of the bio-molecule (L-cysteine) as the capping agent enhances the formation of metallic Cu NPs along with reduction in size, as has been previously observed in the case of gold NPs [39].

The key factor for effective fictionalization and greater stability of NPs depends on the pH of the solution. Effect of pH on the colloidal stability of the Cyst-Cu NPs was shown by changes in LSPR shape and size registered in the pH range of 4.7–7.7 along with prevention of strong basic medium to resist the formation of Cu oxide [40]. It is known that the exact position of the LSPR band depends on variety of factors including size of particles, shape, capping agent, composition and aggregation state of the particles assemblies [41]. However, in this case variation in the pH of solution might have affected the protonation or de-protonation of the acidic group in the L-cysteine structure resulting in the observed changes in the LSPR band. Fig. S1(d) portrays that increase in pH value from 4.7 to 7.7 results in altering the shape of LSPR band from broad to narrow with slight shift in wavelength. The color of colloidal sol also darkens at a lower pH as depicted by digital photograph in the inset figure. Based on these experimental results pH 6.5 was selected as optimum working pH for Cyst-Cu NPs. The blue-shift in LSPR band position ⩾pH 5 (above the isoelectric pH 5.07) confirms the loss of dissociable proton from ammonium moiety of L-cysteine structure as a consequence of which electrostatic repulsions between the negatively charged ($-COO^-$) group of the surface-binded L-cysteine molecules exist and the formation of aggregates is hindered [42,43]. Also, at lower pH values hydrogen bonding between protonated ($-COO^-$) and ($-NH_2$) groups accounts for the broadening of Cyst-Cu NPs LSPR band [42]. Visible spectral profile in connection to the stability of Cyst-Cu NPs with time was recorded and is presented in Fig. S1(e). No change in wavelength and color of colloidal sol was observed even after several weeks of synthesis. Previous research has shown that Cu NPs do not change in an inert atmosphere. In the presence of oxygen dissolved in the aqueous solution, the Cu NPs concentration and the intensity of the LSPR peak gradually decreased as a result of oxidation [9]. In the present study, however, absorption intensity remained unchanged for more than a month after formation and no precipitation and oxidation occurred. This indicates that the Cu NPs are very stable in aqueous solution in the presence of cysteine and hydrazine in a capped test tube.

3.2. Fourier transforms infrared spectroscopy (FTIR)

Interaction of Cu metal surface with L-cysteine molecules was studied using FTIR spectroscopy. L-cysteine being an amino acid subsists as a zwitterion and exhibits bands corresponding to very broad ($-NH_3^+$) stretching, asymmetric/symmetric (–NH) bending, and asymmetric/symmetric carboxylate ion ($-COO^-$) stretching as characteristic vibrations for both primary amine and carboxylate salt. Fig. 1(a, b) shows the FTIR spectrum of pure L-cysteine and Cyst-Cu NPs respectively.

The characteristic bands in Fig. 1(a) can be labeled as: asymmetric and symmetric stretching of (COO^-) at 1630 and 1390 cm^{-1} respectively, (–NH) bending vibration at 1530 cm^{-1} and the very broad band of ($-NH_3^+$) stretching observed in the 3000–3500 cm^{-1} range. In addition, to these a weak band attributed to (–SH) group of cysteine molecule was observed near 2500 cm^{-1}. These results are in good agreement with IR study of a typical amino acid [45–47]. The FTIR spectrum of Cyst-Cu NPs (Fig. 1(b)) illustrates nearly similar vibrational bands however the

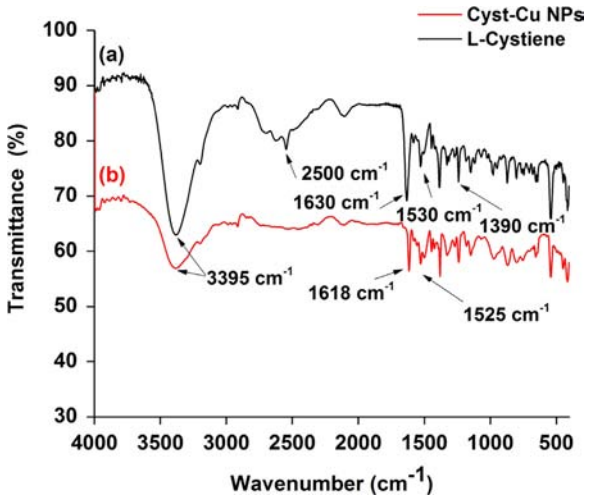

Fig. 1. FTIR spectrum of (a) pure L-cysteine, and (b) L-cysteine functionalized-Cu NPs.

band due to (–SH) as true in case of Fig. 1(a) was not observed in this spectrum which confirms the S–Cu interaction. This observation is further strengthened when one considers the shift in the vibration frequency of carbonyl (COO^-) stretching from 1630 cm^{-1} to 1618 cm^{-1} in the spectrum of Cyst-Cu NPs, indicating interaction between acid group and other cysteine monomers possibly via hydrogen bonding [48]. In addition, slight shifts in frequencies for other groups in spectrum of Cyst-Cu NPs may be explained on the basis of change in dipole as a consequence of L-cysteine binding on high electron dense metal surface [49].

3.3. X-ray powdered diffractometry (XRD)

The X-Ray diffractograms were recorded for phase composition of both L-cysteine functionalized copper nanoparticles and aggregated product collected at the end of colorimetric assay. Fig. 2 (a) represents the XRD patterns for pure Cyst-Cu NPs with characteristic miller indices (111), (200) and (220) lattice planes indexed for face centered cubic structure (FCC) observed at 40.9°, 47.8° and 75.3°. The data in Fig. 2(a) is referred to pure Cu NPs with no peaks indexed to copper oxide. However, final product (Fig. 2 (b)) obtained after exposing Cyst-Cu NPs to excess of Hg^{+2} ions is presented as Cu_2O with indices 29.5°, 36.4°, 42.2°, 1.3°, 73.5° and 77.3° corresponding to (110), (111), (200), (220),(311) and (222) crystal planes. The formation of Cu_2O was expected, as the capping molecules exile the surface and oxidation would occurs which is evident by the gradual decline in the intensity of the LSPR band of Cyst-Cu NPs. The obtained results are in good agreement for both Cu and its oxide with previous studies [11,46,50–52].

3.4. Colorimetric sensing of mercuric ion

Typically, the colloidal sol of Cu NPs exhibits brick red color owing to its LSPR band position of around 400–600 nm [9]. The visible spectrum of the Cyst-Cu NPs is presented in Fig. 3(a). As can be seen, the characteristic LSPR band resides at 565 nm with a narrow band shape, confirming the crystalline nature and uniform particle distribution within the aqueous medium. Similar to SPR which is sensitive to bulk refractive index changes near metal particle surface causing a shift in resonance angle, LSPR is simply measure of an excitation (absorption+scattering) peak shift or change. However in comparison to SPR, the LSPR is much more sensitive towards refractive index changes in the close vicinity of the NP surface due to closely confined optical near field effect thus, allowing it to facilitate real time and on-site analyses [2].

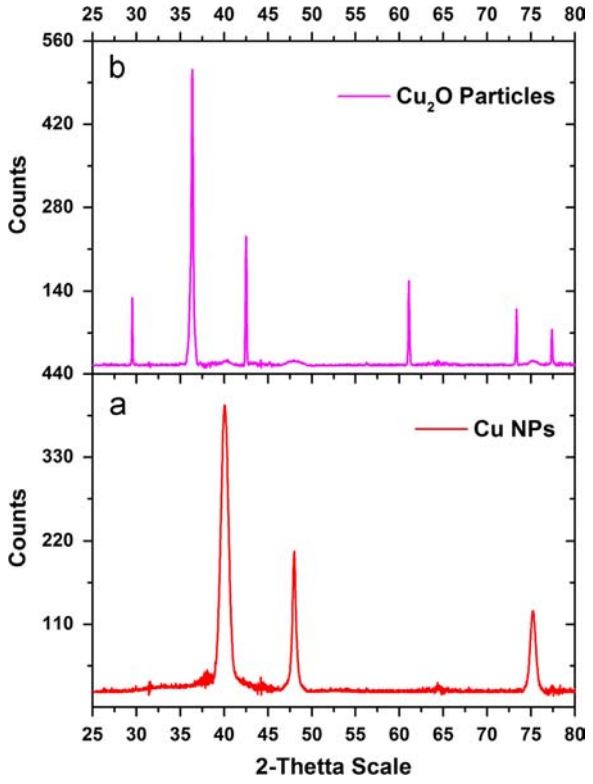

Fig. 2. XRD patterns: (a) cyst-Cu NPs, and (b) Hg^{2+} induced aggregated particles.

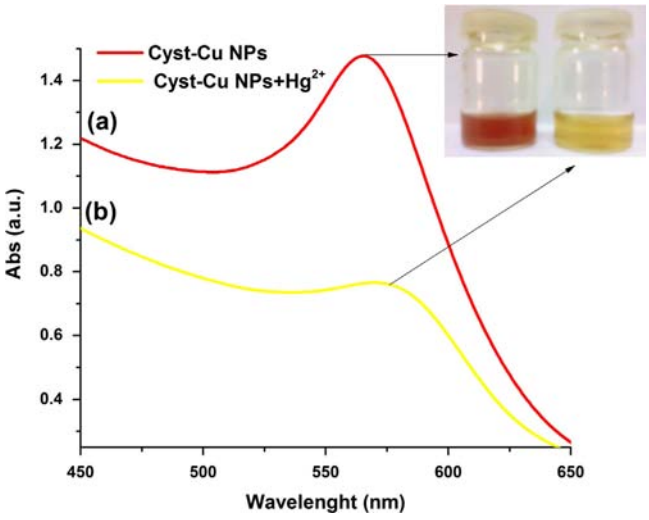

Fig. 3. Visible spectral profile: (a) Cyst-Cu NPs, and (b) Cyst-Cu NPs+Hg^{2+}. (For interpretation of the references to color in this figure, the reader is referred to the web version of this article.)

In case of interaction of Cyst-Cu NPs with Hg^{2+} ions, a colorimetric change from brick red (Fig. 3(a)) to pale yellow (Fig. 3(b) corresponding to change in the spectral profile of Cyst-Cu NPs from narrow, blue-shifted band to broader and red-shifted band with decreased intensity was observed as illustrated in Fig. 3. The change in spectral profile after exposure to Hg^{2+} can be explained on the basis of aggregation of particles within the aqueous solution.

The visual insight regarding morphological changes based on non-aggregated and aggregated forms of Cu NPs was obtained by the TEM imaging technique. It was observed that in the absence of Hg^{2+}, the Cyst-Cu NPs formed were spherical and well dispersed with an average particle size of 34 ±2.1 nm ranging from 10 to

108 nm size as depicted in Fig. 4(a, b). These morphological features are in good agreement with the LSPR band of Cyst-Cu NPs observed in Fig. 3(a). The present scenario clearly reflects that the interaction between the bio molecules (L-cysteine) and surface of Cu NPs was sufficient enough for the formation of stable, spherical nanoparticles. In contrast to this TEM images in Fig. 4 (c, d) obtained at same scale size after the interaction of Cyst-Cu NPs with Hg^{2+} ions (3.5 μM and 4.0 μM) illustrates the formation

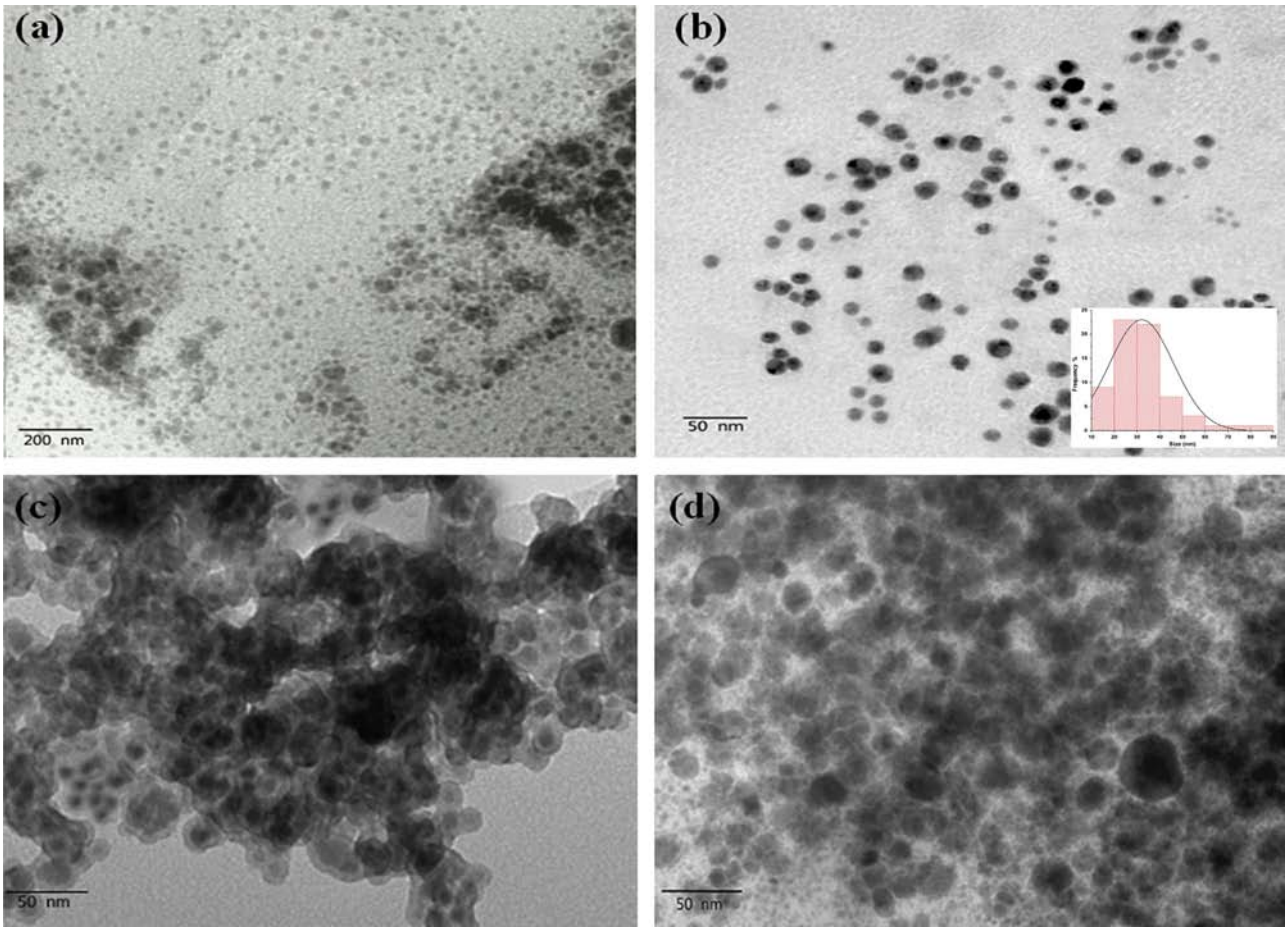

Fig. 4. TEM micrographs of Cyst-Cu NPs: (a) low resolution, (b) high resolution, (c) Cyst-Cu NPs + 3.5 μM Hg^{2+}, and (d) Cyst-Cu NPs + 4.0 μM Hg^{2+}.

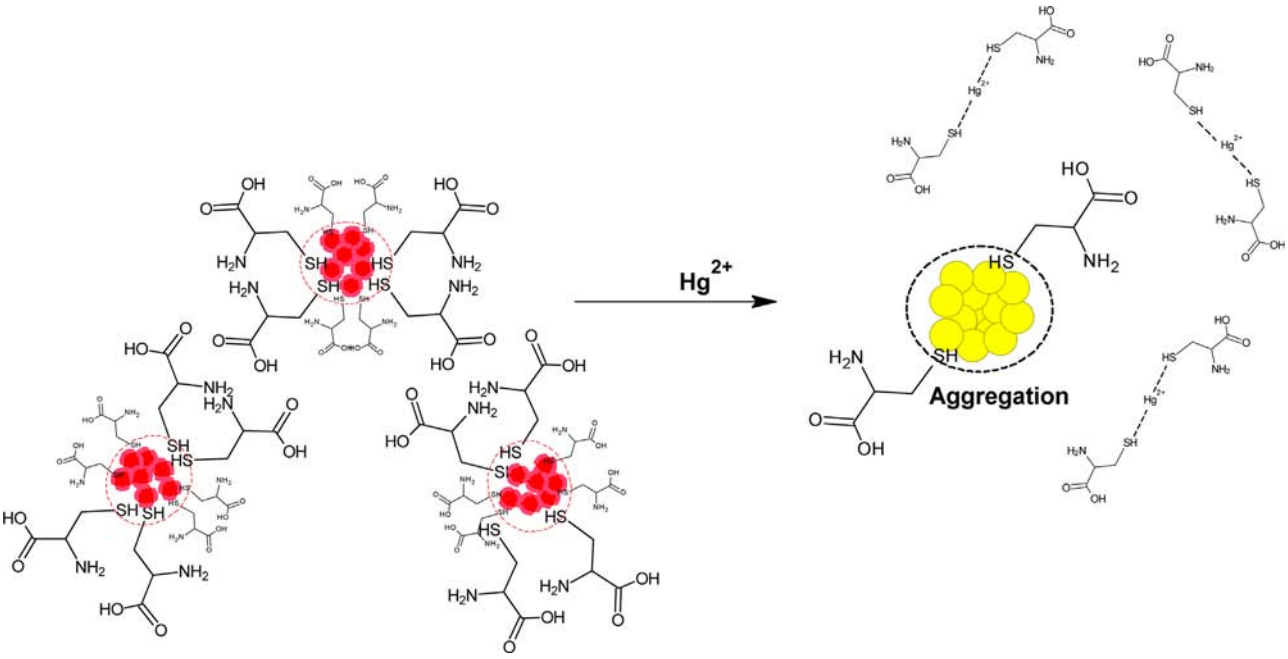

Scheme 1. Hg^{2+} induced aggregation of Cyst-Cu NPs.

of very large aggregates ⩾100 nm, with high degree of twining and fusion. Generally, face-centered cubic (FCC) structured metallic nanocrystals have a tendency to nucleate and grow into twinned particles with their surfaces surrounded by the lowest energy facets [40]. Thus, such growth accounts for the decrease intensity and change in the LSPR shape of Cyst-Cu NPs.

Based on these images, a mechanism for aggregation of particles is presented in Scheme 1. We believe that the change in LSPR shape and size is a consequence of detachment of L-cysteine molecules from the surface of Cyst-Cu NPs, allowing well dispersed small nanoparticles to grow into larger aggregates due to fusion of un-capped particles, which are incapable of producing surface plasmons according to the Mie theory [53]. In the presence of oxygen dissolved in the aqueous solution, the Cu NPs concentration and the intensity of the LSPR band gradually decreased as a result of oxidation [5,54]. The hypothesis is further supported by the increased peak intensities indexed to Cu_2O in the XRD patterns obtained at different concentrations of mercuric ion (Fig. (S3)). These results indicate gradual oxidation of Cyst-Cu NPs with increasing concentration of Hg^{2+} ions. Thus, excess of Hg^{2+} ion would provide a very little or no opportunity to L-cysteine to bind with the metallic surface of Cu, owing to its high thiophilicity compared with other metal cations leading to complete conversion of metallic copper to copper oxide in aqueous solution which was confirmed from XRD pattern shown in Fig. 2(b). In addition decrease in zeta potential measurement (Fig. S2(a, b)) of well-dispersed Cyst-Cu NPs from about −23 mV to −13 mV after Hg^{2+}-induced aggregation further strengthens our hypothesis of Hg^{2+}-induced loss of ligands from the surface of Cu NPs.

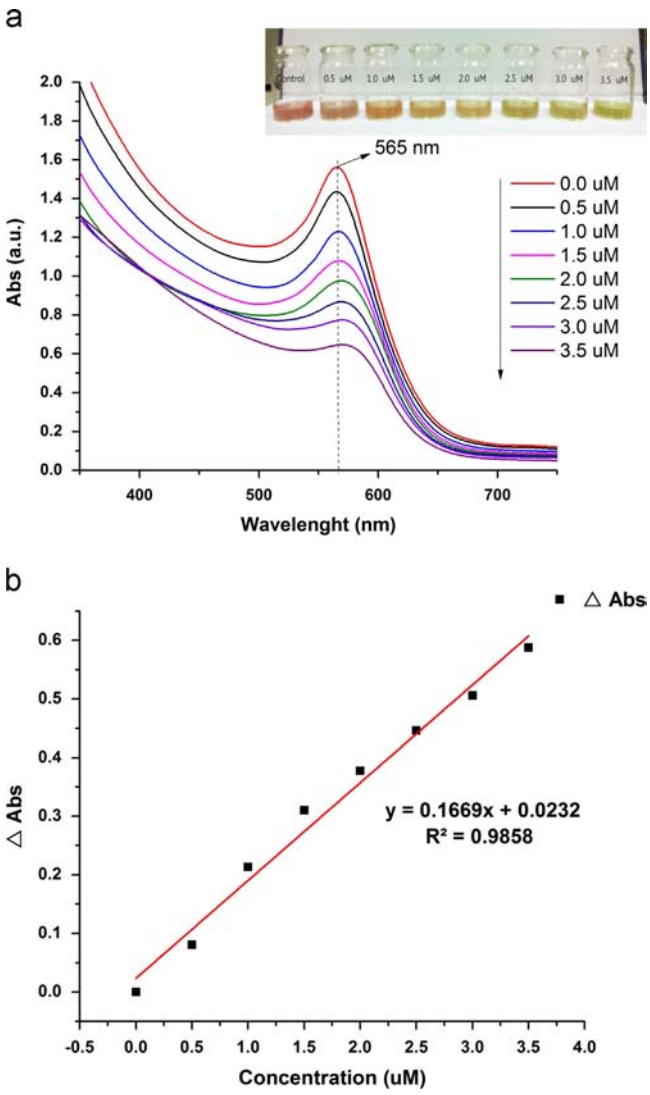

Fig. 5. (a) Decline in the LSPR abs with increasing concentration of Hg^{2+} (b) linear regression plot between ΔA (LSPR) and Hg^{2+} concentrations.

More experiment showed that the decline in the intensity of LSPR band (or ΔA) is proportional to the Hg^{2+} concentration. So the present work represents a novel, simple, selective, economic and fast colorimetric method for determination of Hg^{2+} in aqueous solution using L-cysteine functionalized Cu NPs.

3.5. Analytical performance of colorimetric assay

Quantitative response based on colorimetric assay was obtained by monitoring the changes in the ΔA (LSPR) band of Cyst-Cu NPs in the spectral range of 400–800 nm (Fig. 5(a)) upon addition of Hg^{2+} ions. The useful analytical data was obtained by Linear regression analysis of ΔA (LSPR) at 565 nm plotted against Hg^{2+} concentrations. The method showed good linearity in the calibration range 0.5×10^{-6}–3.5×10^{-6} mol L^{-1} of Hg^{2+} ions (Fig.5(b)). The correlation of determination (r^2) was 0.9882, with limit of detection and quantification calculated to be 4.30×10^{-8} and 0.1×10^{-a} mol L^{-1} respectively. The LOD and LOQ were determined from three times the standard deviation of the blank signal ($3\times\partial$/slope), and ten times the standard deviation of blank signal ($10\times\partial$/slope) respectively.

Table 1 presents the comparative data of limit of detection by various types of Ag and Au based sensor regarding the detection of Hg^{2+} ions. The table shows that the newly developed Cyst-Cu NPs based colorimetric sensor for Hg^{2+} ions in our case produced better results than several of the reported sensors with the best advantage of high economy.

3.6. Selectivity of sensor

To test the selectivity of Cyst-Cu NPs for other metal ions, we investigated the colorimetric response in the presence of various metal ions including Pb^{2+}, Ca^{2+}, Co^{2+}, $Zn^{2+}Mg^{2+}$, Ni^{2+}, Ag^{+}, and Cd^{2+} ions at the concentration of 10 μM. These metals were

Table 1
Comparison of L-cysteine functionalized Cu NPs as a colorimetric sensor for the detection of Hg^{2+} with previously reported methods.

No.	Sensor System	Limit of Detection (LOD) M	References
1.0	p-PDA functionalized Ag NPs	8.01×10^{-7}	[28]
2.0	Unmodified Ag NPs	2.2×10^{-6}	[8]
3.0	Mesna modified Ag NPs	2.4×10^{-9}	[56]
4.0	Tween 20-modified Au NPs	1.0×10^{-7}	[57]
5.0	L-cysteine functionalized Au NPs	1.0×10^{-7}	[58]
6.0	Mercaptopropionic acid-modified	1.0×10^{-7}	[59]
7.0	Poly(diallyldimethylammonium) chloride (PDDA)-coated Au NPs	2.5×10^{-8}	[60]
8.0	L-cysteine functionalized Cu NPs	4.3×10^{-8}	This Study

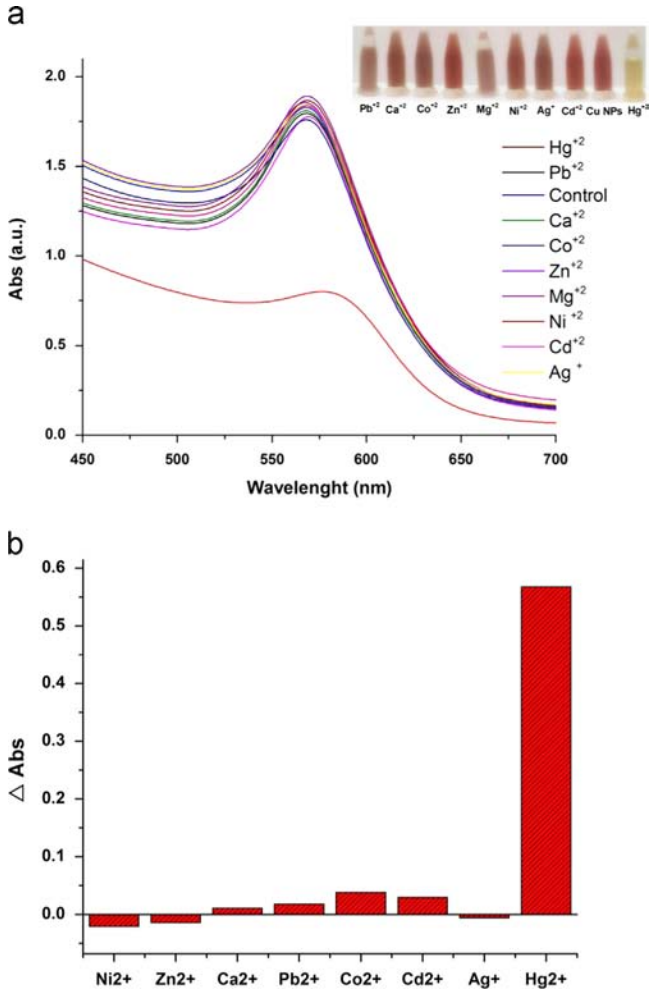

Fig. 6. (a) Visible spectral profile demonstrating selectivity of cyst-Cu NPs for Hg^{2+}, (b) bar diagram exhibiting magnitude of change ΔA (LSPR) for various cations.

added into 3 mL of Cyst-Cu NPs solution under the same conditions as true for Hg^{2+} ions. The selectivity of sensor can be visualized with naked eye as represented by the inset picture in Fig. 6(a); upon interaction of freshly prepared Cyst-Cu NPs with various metal ions, the only solution containing Hg^{2+} ions shows changes from red to pale yellow, while the effect of the other metal ions on the color and LSPR band of Cyst-Cu NPs solution is negligible, indicating that the developed sensor has very high selectivity toward Hg^{2+} ions. Fig. 6(b) represents the bar diagram for selectivity of the sensor. Slight variation in the LSPR of Cyst-Cu NPs upon addition of metal ions could be ascribed as a result of slight change in local refractive index at the interface between Cyst-Cu NPs and solution. However, increased intensities and narrowness in LSPR of Cyst-Cu NPs for some metal cations can be described as consequence of non-uniform absorption and variable sizes of these ions, leading to a layer surrounding the copper nanoparticles and changing dielectric medium near nanoparticles [61,62]

The excellent selectivity of this model can be ascribed as a consequence of higher stability constants (log Kf) of Hg (cysteine) ca. 43.5 compared to other metal cations like Pb^{2+}, Co^{2+}, Mg^{2+}, Ni^{2+}, Cd^{2+}, Ag^{+} and Zn^{2+} ions are 12, 16, 4, 19, 7.83, 12.7, 18 respectively [63].

3.7. Application of developed sensor to real water samples

Samples of water from various localities of the river Sindh near Kotri barrage were subjected for Hg^{2+} ions determination using the developed sensor based on LSPR of Cyst-Cu NPs. The samples were treated after proper dilution in order to bring the final Hg^{2+} ions concentration in the linear range of the sensor. The linear relation in Fig. 5(b) was used for the determination of mercury ion content in river water samples. According to final results, the Hg^{2+} ions in the river sample was found to be in range between 5.9 μM and 6.3 μM as presented in table 2. The result shows very high mercury content, above the EPA criterion of 0.002 mg/L (equivalent to 0.009 μM or 2 ppb) set to protect public health [64].

Table 2
Determination of mercuric ions in real water samples collected from Sindh River near Kotri Barrage, Jamshoro, Pakistan.

Samples	Concentration (μM)[n]	Relative standard deviation (%)
Sample 1	6.3	0.8
Sample 2	5.9	0.6
Sample 3	6.1	1.1

Conditions: 3 mL Cyst-Cu NPs solution, 10 μl real sample (2 times diluted), no. of replications=3 and reaction time: 2–3 min.

4. Conclusion

In conclusion, L-cysteine was utilized as a greener protecting or functionalizing agent for the synthesis of stable Cu NPs. The synthesis of stable Cyst-Cu NPs was made possible with the help of using hydrazine as the reducing agent which provided sufficient N_2 and hence avoided the use of inert gas from outside source. This approach is simple, cost effective and provides efficient route for preparation of stable Cu NPs in aqueous medium. Furthermore, these stable Cyst-Cu NPs were used as simpler, easily implemented, highly sensitive, extremely selective and highly economic colorimetric sensor for Hg^{2+} determination based on change in LSPR upon addition of various concentrations of Hg^{2+} ions to colloidal sol. The secret of sensor is based upon the conversion of stable Cyst-Cu NPs to un-protected Cu_2O NPs after addition of Hg^{2+} ions which remove the protective layer of L-cysteine around Cu NP resulting in aggregated NPs with sufficient change in LSPR property. The successful application of sensor in real water samples with sensitive Hg^{2+} ions detection based on colorimetric and naked eye examination proves its feasibility in all types of waters and it could be transformed into detection strips for rapid detection of mentioned ions. In comparison to precious metal sensors for Hg^{2+} ions detection, the currently developed sensor based on Cu NPs is not only highly sensitive and efficient by it cost effective nature make it far more superior to the mentioned sensors.

Acknowledgments

We acknowledge the Higher Education Commission, Islamabad, Pakistan for provision of financial assistance during this research. The authors equally highly thank and cordially appreciate the financial support by King Saud University for provision of funding via their Research Project no. RGP-VPP-236.

Appendix A. Supplementary materials

Supplementary data associated with this article can be found in the online version at http://dx.doi.org/10.1016/j.talanta.2014.07.023.

References

[1] S. Zhu, F. Li, C. Du, Y. Fu, Sens. Actuators B: Chem. 134 (2008) 193–198.
[2] E. Kazuma, T. Tatsuma, Nanoscale 6 (2014) 2397–2405.
[3] S.L. Smitha, K.M. Nissamudeen, D. Philip, K.G. Gopchandran, Spectrochim. Acta A 71 (2008) 186–190.
[4] S. Eustis, M.A. El-Sayed, Chem. Soc. Rev. 35 (2006) 209–217.
[5] S.-H. Wu, D.-H. Chen, J. Colloid Interface Sci. 273 (2004) 165–169.
[6] S. Sun, C. Kong, D. Deng, X. Song, B. Ding, Z. Yang, CrystEngComm 13 (2011) 63–66.
[7] H.K. Sung, S.Y. Oh, C. Park, Y. Kim, Langmuir 29 (2013) 8978–8982.
[8] K. Farhadi, M. Forough, R. Molaei, S. Hajizadeh, A. Rafipour, Sens. Actuators B: Chem. 161 (2012) 880–885.
[9] A. Hatamie, B. Zargar, A. Jalali, Talanta 121 (2014) 234–238.
[10] M. Vaseem, K.M. Lee, D.Y. Kim, Y.-B. Hahn, Mater. Chem. Phys. 125 (2011) 334–341.
[11] D. Lai, T. Liu, G. Jiang, W. Chen, J. Appl. Polym. Sci. 128 (2013) 1443–1449.
[12] D. Zhang, H. Yang, Physica B 415 (2013) 44–48.
[13] A.P. de Silva, D.B. Fox, A.J.M. Huxley, T.S. Moody, Coord. Chem. Rev. 205 (2000) 41–57.
[14] G.W.F.A. Cotton, C.A. Murillo, M. Bochmann, New York, John Wiley & Sons, 6th ed., 1999.
[15] P.B. Tchounwou, W.K. Ayensu, N. Ninashvili, D. Sutton, Environ. Toxicol. 18 (2003) 149–175.
[16] T.W. Clarkson, L. Magos, G.J. Myers, N. Engl. J. Med. 349 (2003) 1731–1737.
[17] Y. Wang, F. Yang, X. Yang, Biosens. Bioelectron. 25 (2010) 1994–1998.
[18] C.J. de Castro Maciel, G.M. Miranda, D.P. de Oliveira, M.E.P.B. de Siqueira, J.N. Silveira, E.M.A. Leite, J.B.B. da Silva, Anal. Chim. Acta 491 (2003) 231–237.
[19] R.F. Suddendorf, J.O. Watts, K. Boyer, J. Assoc. Anal. Off. Chem. 64 (1981) 1105–1110.
[20] Q. Yang, Q. Tan, K. Zhou, K. Xu, X. Hou, J. Anal. At. Spectrom. 20 (2005) 760–762.
[21] B.M. Fong, T.S. Siu, J.S. Lee, S. Tam, J. Anal. Toxicol. 31 (2007) 281–287.
[22] D. Karunasagar, J. Arunachalam, S. Gangadharan, J. Anal. At. Spectrom. 13 (1998) 679–682.
[23] S. Ichinoki, N. Kitahata, Y. Fujii, J. Liquid Chromatogr. Relat. Technol. 27 (2004) 1785–1798.
[24] J.J. Nevado, R.C. Martin-Doimeadios, F.J. Bernardo, M.J. Moreno, J. Chromatogr. A 1093 (2005) 21–28.
[25] B. Kuswandi, Nuriman, H.H. Dam, D.N. Reinhoudt, W. Verboom, Anal. Chim. Acta 591 (2007) 208–213.
[26] A. Fan, Y. Ling, C. Lau, J. Lu, Talanta 82 (2010) 687–692.
[27] J.N. Solanki, R. Sengupta, Z.V.P. Murthy, Solid State Sci. 12 (2010) 1560–1566.
[28] S. Bothra, J.N. Solanki, S.K. Sahoo, Sens. Actuators B: Chem. 188 (2013) 937–943.
[29] D. Liu, W. Qu, W. Chen, W. Zhang, Z. Wang, X. Jiang, Anal. Chem. 82 (2010) 9606–9610.
[30] N.H. Kalwar, Sirajuddin, S.T.H. Sherazi, A.R. Khaskheli, K.R. Hallam, T.B. Scott, Z.A. Tagar, S.S. Hassan, R.A. Soomro, Appl. Catal. A 453 (2013) 54–59.
[31] N.H. Kalwar, Sirajuddin, T.H. Sherazi, Z.A. Tagar, A.R. Khaskheli, Y. Hassan, S.S. Junejo, Pak. J. Anal. Environ. Chem. 14 (2) (2013) 54–60.
[32] C. Noguez, J. Phys. Chem. C 111 (2007) 3806–3819.
[33] M.A.V.T Ghodselahi, A Shafiekhani, Physica B 42 (2009) 015308.
[34] M. Abdulla-Al-Mamun, Y. Kusumoto, M. Muruganandham, Mater. Lett. 63 (2009) 2007–2009.
[35] F. Chen, N. Alemu, R.L. Johnston, AIP Adv. 1 (2011) 032134–032149.
[36] S.K. Ghosh, T. Pal, Chem. Rev. 107 (2007) 4797–4862.
[37] S. De, S. Mandal, Colloid Surf. A 421 (2013) 72–83.
[38] B.K. Park, S. Jeong, D. Kim, J. Moon, S. Lim, J.S. Kim, J. Colloid Interface Sci. 311 (2007) 417–424.
[39] Z. Zhong, A.S. Subramanian, J. Highfield, K. Carpenter, A. Gedanken, Chem. Eur. J. 11 (2005) 1473–1478.
[40] T.M.D. Dang, T.T.T. Le, E. Fribourg-Blanc, M.C. Dang, Adv. Nat. Sci.: Nanosci. Nanotechnol. 2 (2011) 015009.
[41] M.J. Guajardo-Pacheco, J.E. Morales-Sánchez, J. González-Hernández, F. Ruiz, Mater. Lett. 64 (2010) 1361–1364.
[42] E. Csapó, R. Patakfalvi, V. Hornok, L.T. Tóth, Á. Sipos, A. Szalai, M. Csete, I. Dékány, Colloid Surf. B 98 (2012) 43–49.
[43] A. Mocanu, I. Cernica, G. Tomoaia, L.-D. Bobos, O. Horovitz, M. Tomoaia-Cotisel, Colloid Surf. A 338 (2009) 93–101.
[45] A. Barth, Biochim. Biophys. Acta 1767 (2007) 1073–1101.
[46] S. Panigrahi, S. Kundu, S. Basu, S. Praharaj, S. Jana, S. Pande, S.K. Ghosh, A. Pal, T. Pal, ASC. Symp. Ser. 17 (2006) 5461.
[47] Sirajuddin, A. Nafady, H.I. Afridi, S. Sara, A. Shah, A. Niaz, J. Iran. Chem. Soc. 8 (2011) S34–S43.
[48] M.M.K. Khan, K. Shafeer, Jin-Tae Lee, Moo-Hwan Cho, Bull. Korean Chem. Soc. 33 (2012) 2592–2596.
[49] Z.-X. Cai, H. Yang, Y. Zhang, X.-P. Yan, Anal. Chim. Acta 559 (2006) 234–239.
[50] S. Qiu, J. Dong, G. Chen, J. Colloid Interface Sci. 216 (1999) 230–234.
[51] Y. Abboud, T. Saffaj, A. Chagraoui, A. Bouari, K. Brouzi, O. Tanane, B. Ihssane, Appl. Nanosci. (2013) 1–6.
[52] A. Nowak, J. Szade, E. Talik, A. Ratuszna, M. Ostafin, J. Peszke, Mater. Chem. Phys. 145 (2014) 465–470.
[53] N. Vasimalai, G. Sheeba, S.A. John, J. Hazard. Mater. 213–214 (2012) 193–199.
[54] M. Grouchko, A. Kamyshny, K. Ben-Ami, S. Magdassi, J. Nanopart. Res. 11 (2009) 713–716.
[56] Y. Chen, L. Wu, Y. Chen, N. Bi, X. Zheng, H. Qi, M. Qin, X. Liao, H. Zhang, Y. Tian, Microchim Acta 177 (2012) 341–348.
[57] C.-Y. Lin, C.-J. Yu, Y.-H. Lin, W.-L. Tseng, Anal. Chem. 82 (2010) 6830–6837.
[58] F. Chai, C. Wang, T. Wang, Z. Ma, Z. Su, ACS Symp. Ser. 21 (2010) 025501.
[59] C.-C. Huang, H.-T. Chang, Chem. Commun. (2007) 1215–1217.
[60] C.J. Yu, C.Y. Lin, C.H. Liu, T.L. Cheng, W.L. Tseng, Biosens. Bioelectron. 26 (2010) 913–917.
[61] Yap Wing Fen, W. Mahmood Mat Yunus, Opt. Photonics J. 1 (2011) 116–123.
[62] Jyoti Boken, Dinesh Kumar, Int. J. Res. Dev. 4 (2014) 303–308.
[63] R.N. Patel, N. Singh, R.P. Shrivastava, K.K. Shukla, P.K. Singh, J. Chem. Sci. 114 (2002) 115–124.
[64] Jesse M. Lepak, Hannah A. Shayler, Clifford E. Kraft, Barbara A. Knuth, Bioscience 59 (2) (2009) 174–181.